Chapter 7

Neuroanatomical Circuit Based Drug Repurposing in Alzheimer's Disease

Chapter 7

7. Neuroanatomical Circuit Based Drug Repurposing in different biological sub-types of Alzheimer's Disease

7.1 Introduction

This study aims to clinically validate our previous research on hepatotropic drugs that enhance the clearance of brain amyloid beta through liver into bile and feces. Through tractography analysis, we formulated a functional basis of the Braak microscopy-based staging of spreading amyloid deposition pattern in the brain and our tractography analysis showed that tracts associated with the spreading Braak stages were primarily involved in limbic, frontal and parietal networks. Our predicted hepatotropic drugs also improved these networks that were compromised in Alzheimer's patients. Our analysis offers a clinical endorsement of the effectiveness of repurposed medications against Alzheimer's disease that we predicted from the systems biology analysis.

Our current study aims to identify the diffusivity parameters in the aforementioned brain networks which are affected by Alzheimer's disease and are relevant to the drug treatments. The white matter integrity of the tracts was evaluated in AD and compared to control healthy subjects. White matter degeneration could be an early marker of AD pathogenesis and therapeutic intervention may also improve the above-mentioned affected regions. Analysing the alterations in the microstructural organization of the regions of interest (ROIs) may be helpful in AD diagnosis. Moreover, we can thus implicate that hepatotropic drugs may have worthwhile potentiality as AD therapeutic modality with indicative clinical corroborations as furnished above.

Our present investigation has also shown that the three hepatomodulative drugs (Metformin, Cilostazol and Rifampicin) may be respectively efficacious for the frontal, temporal and parietal subtypes of the alzheimer's disease.

7.2 Materials and methods

7.2.1 Analysis of clinical trial findings and neuroimaging scans

We have analysed the clinical findings and neuroimaging scans of three separate clinical trials of AD using those three hepatomodulatory amyloid-clearance drugs (metformin [68]/cilostazol [69]/rifampicin [65]). According to the images, we observe that these three drugs stimulate different brain regions in AD patients, with the dominant activation respectively being in three zones: (i) Segment-1: Metformin activates the orbitofrontal and uncinate region [68]; (ii) Segment-2: Cilostazol activated the parietal and inferofrontal region [69]; (ii) Segment-3: Rifampicin activated the posterior cingulate and parietal association area [65].

7.2.2 DTI Data acquisition

The Alzheimer's Disease Neuroimaging Initiative (ADNI) database was used to obtain structural MRI and DTI data for cognitively normal (CN) and Alzheimer disease (AD) subjects used in the present study [142]. The ADNI program was launched in 2004 as an multicentric clinical cooperation as a private-public partnership. The principal objective of this initiative was to develop clinical, imaging, genetic, and biochemical biomarkers for the early detection and monitoring of AD. We have analyzed diffusion MRI scans from the ADNI database (http://adni.loni.usc.edu) of 5 healthy controls and 5 AD subjects.The subjects were classified using mini-mental state evaluation (MMSE) and global clinical dementia rating (CDR) scores [143]. ADNI control participants (healthy subjects) had Mini-Mental Status Examination (MMSE) scores of 24-30 and a Clinical Dementia Rating (CDR) score of 0. Similarly, for Alzheimer's subjects, MMSE score was

between 20-26 and CDR of 0.5-1.0. The Institutional Review Board approved this study of all the participants. Informed written consent was obtained from all subjects. We included subjects whose baseline DWI and T1-weighted MRI scans were accessible. For all participants, whole-brain MRI scanning was performed using a range of various 3T Medical Systems made by GE, Siemens, and Philips. For each DTI scan, two sets of ten images were obtained: ten diffusion-weighted images (b = 1000 s/mm2) and ten T1-weighted images without diffusion stimulation (b0 images). Two distinct acquisition protocols are outlined for DWI scans: According to the "IDA_MR_Metadata_Listing.csv" file on the ADNI website, 1) Axial DTI and 2) Enhanced Axial DTI. On ADNI's main website, you can find more information about the data acquisition procedures for its MRI scanners.

7.2.3 Tractography Analysis

The diffusion MRI data were pre-processed with the DSI-Studio software. This platform is used for deterministic fibre tracking, reconstruction, and three-dimensional visualisation (http://dsi-studio.labsolver.org). The restricted diffusion was measured using restricted diffusion imaging. The diffusion data were reconstructed using generalised q-sampling imaging (GQI) with a diffusion sampling length ratio of 1.25. The tensor metrics were computed. A deterministic fibre tracking algorithm was used. To obtain the tracts, a ROI was placed at themetformin affected regions: Uncinate Fasciculus and Orbitofrontal Cortex[68]; cilostazol affected regions:Inferior Frontal Gyrus, and Parietal lobes [69]; and rifampicin affected regions: Parietal Association Cortex and Posterior Cingulate Cortex [65]. The anisotropy threshold was 0.02. The angular threshold was 60 degrees. The step size was 0.1 mm. Tracks with length shorter than 5 or longer than 300 mm were discarded [144].To know the anatomical structure of the findings, we have used findings as ROIs by [Tracts][Tracts to ROI] to run fiber tracking and then used

[Tracts][Miscellaneous][Recognize Track] to determine the anatomical structures. Tract metrics were also obtained using [Tracking Parameters] [Differential Tracking] [Metrics] option of DSI studio.

7.2.4 Genetic Association Analysis

Microarray data for Alzheimer's Disease genes proposed in our hypothesis (ABCG2, ABCB11, ABCA1, MDR1, SCD and ASBT) in post-mortem human brain tissue of the normal adults were downloaded from the human brain transcriptome database of the Allen Brain Atlas (https://human.brain-map.org/). Microarray survey, data normalization and platform selection along with the ontology and nomenclature of anatomical structures of brain were mentioned in the allen brain atlas platform (Documentation - Allen Human Brain Atlas (brain-map.org)). The brain regions where upregulation and downregulation of proposed genes occur were identified based on expression levels.

7.3 Results

7.3.1 Clinical trial analysis

Our analysis of the clinical findings and neuroimaging scans revealed the three segments of brain were activated by the proposed drugs. Table 7 represents information of our systems-biology analysis and the clinical trials. Analyzing those above-mentioned scans, we find that these three drugs activate different neural regions in AD patients with the dominant activation being respectively in following three zones. (a) Segment-1: Activation of areas as orbitofrontal and uncinate region by Metformin, thereby improving learning/memory ($p = 0.044$) [68]. In their study Koeing et al. reported increasing orbitofrontal cerebral blood flow after metformin treatment, as estimated by MRI-ASL perfusion study. Their cognitive testing (ADAS-Cog and CANTAB-PAL tests) also revealed improvement in learning and memory as well as in executive functioning in AD subjects after treatment with metformin; (b) Segment-2: The FDG-PET study conducted

by Lee et al. reported that activation of areas as parietal region and inferofrontal region by Cilostazol, with notable glucose metabolism increase ($p = 0.005$) [69]; moreover, psychological testing by ADAS-Cog scoring showed definitive improvement; (c) Segment-3: Iizuka el al. revealed in their FDG-PET analysis that activation of areas as posterior cingulate and parietal association area by Rifampicin, whose metabolic change between 12-and 6-month therapy was markedly enhanced ($p = 0.009$); here cognitive assessment by MMSE showed appreciable affirmative effect [65].

Table 7. Synopsis of our systems biology approach and of collateral clinical trials for pharmacologically enhanced hepatic clearance of amyloid-beta in Alzheimer's disease.

Proposed Hepatomodulative Drugs	Systems Biology Pathway of Amyloid excretion	Dose/Dose regimen	Clinical Investigation	Outcome
Rifampicin	Pregnane-X-receptor	450 mg/d for 12 months	Elderly 40 non-demented patients having mycobacterium infections with impaired AD-type hypo-metabolism	Significant rise in metabolic status of the posterior cingulate cortex between 6 month and 12 month therapy ($p = 0.009$) [65]
Metformin	Bile salt export pump receptor	500 mg weekly until a maximum of 2000 mg across 8 weeks	Placebo-controlled, randomized, 2-month trial in 20 nondiabetic subjects having mild dementia due to AD	Executive functioning enhancement (p=0.033), cerebral perfusion increase in relevant region (p<0.05)[68]
Cilostazol	Phosphodiesterase receptor	50 mg twice daily, increased to 100 mg twice daily, after 2 weeks	Double-blind, randomized, placebo-controlled, 24-week study in AD patients	Significant enhancement in cerebral glucose metabolism ($p < 0.005$) along with improving or protecting cognitive function in AD [69]

Analyzing those scans, we find that these three drugs activate different neural regions in AD patients with the dominant activation being respectively in following three zones.

(a) Segment-1: Activation of areas as orbitofrontal and uncinate region by Metformin, improving learning/memory (p=0.044) [68].

(b) Segment-2: Activation of areas as parietal region and inferofrontal region by Cilostazol, with notable glucose metabolism increase (p=0.005) [69].

(c) Segment-3: Activation of areas as posterior cingulate and parietal association area by Rifampicin, whose metabolic change between 12-and 6-month therapy was markedly enhanced (p=0.009) [65].

7.3.2 Deterministic Tractography

We separately constructed for each segment the fibre tracts using deterministic tractography. Thereafter, we performed the identification and nomenclature of the nerve tracts corresponding to those three segments as follows (Figure 36a-b).

Segment 1: Uncinate fasciculus, anterior thalamocortical radiation, and thalamocerebral (as dentatorubothalamic) tract.

Segment 2: Inferior fronto-occipital fasciculus (IFOF) leading to occipito-patietal region. It is known that IFOP tract also connects parietal lobe and is part of fronto-parietal network [144].

Segment-3: Cingulum's fronto-parietal projections and superior longitudinal fasciculus dorsally.

Anatomically, it is known that the uncinate fasciculus adjoins the entorhinal cortex-EC. Indeed, entorhinal cortex is a most vulnerable region for AD, as it is juxtaposition between allocortex and neocortex, and is the initial area where amyloid is first formed in AD, due to mitophagy-induced death of entorhinal neurons [145]. Accordingly, we can

construe that amyloid spread in brain will initialize in EC and then traverse by the white-matter fibre of uncinate and anterior-thalamic/rubrothalamocerebral tracts (Segment-1).

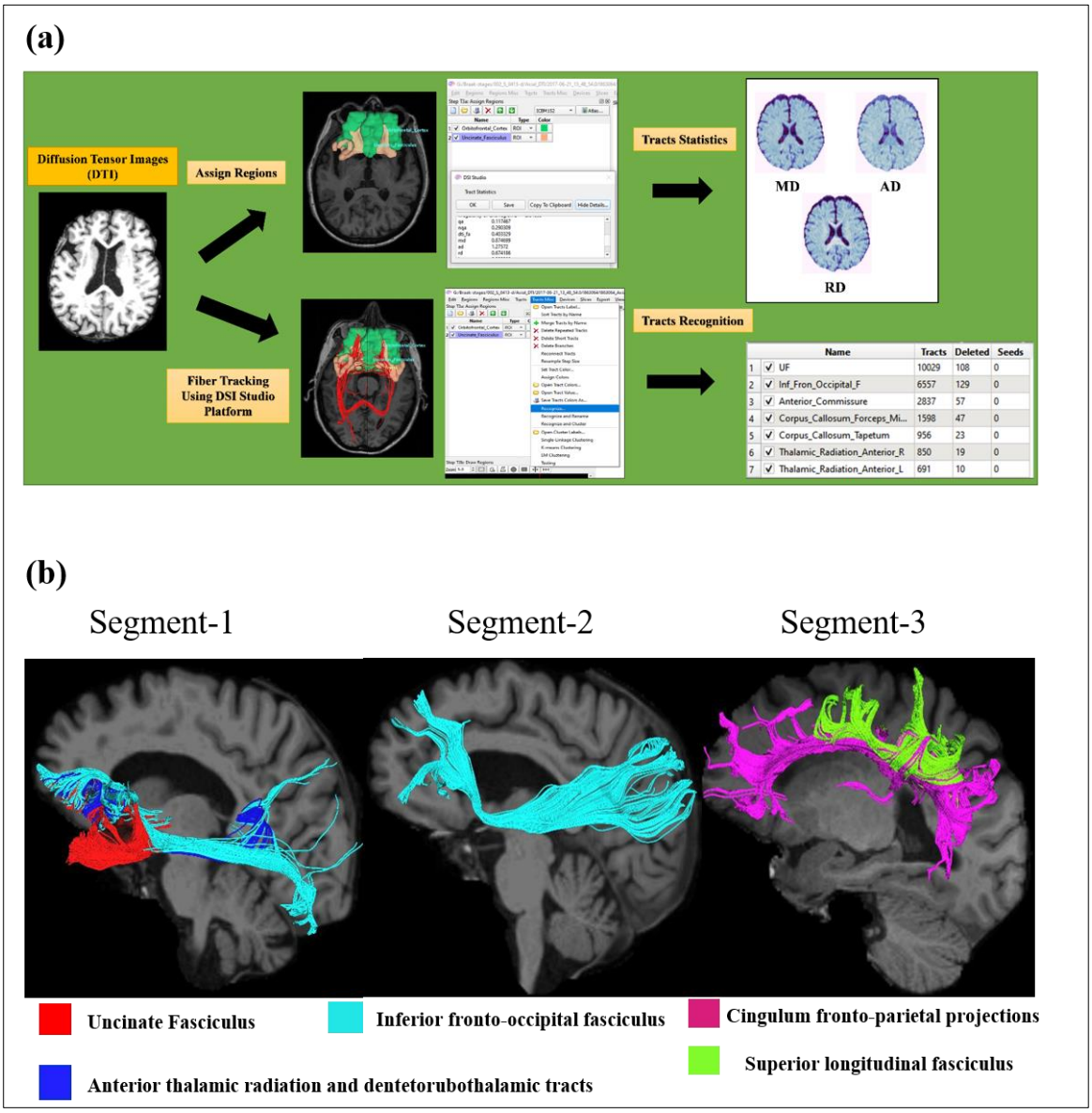

Figure 36: *(a) Imaging analysis procedure for diffusion tensor imaging (b) Tractography and identification of the fibres in the three segments of the brain.*

We now explore the full gamut of amyloid spread via the aforesaid white matter tracts (Figure 36b) and note the segments may enable amyloid spreading via a circumcerebral pattern:

(i) Segment-1: Anterior portion of the tractography from uncinate faciculus, robrothalamocerebral tract and anterior thalamic radiation, leads forward to neocortex region, as orbitofrontal/inferior frontal cortex, and frontal area of anterior cingular region

(ii) Segment-2: Posterior portion of the tractography from inferior fronto-occipital fasciculus leads towards the allocortex region, as the limbic system, e.g. posterior cingular area, and to temporo-occipital-parietal region.

(iii) Segment-3: Tractographic fibre of the superior longitudinal fasciculus and and cingulum's fronto-parietal projection transverse supracallosally and interlink the frontal and occipito-patietal regions of the brain. Indeed, the anterior and posterior cingular fibres (segment-1,2) meet supracallosally around the vertex sensorimotor region.

In other words, the amyloid spread via tracts of the three segments form a circumcerebral route as delineated in Figure 37.

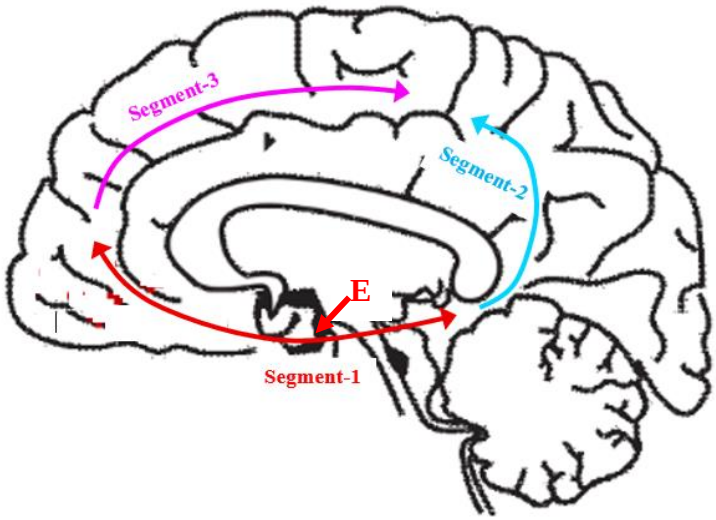

Figure 37: *Geometric motif of the white matter tract profile providing the neural fibre scaffold for amyloid migration circumferentially across the cerebrum, with the three schematic segments shown. The amyloid deposition starts at entorhinal-uncinate region E and migrates bidirectionally as segment-1 and then circles across the cerebrum, by segments 2 and 3.*

7.3.3 Microscopical histological validation with Braak Staging

We now show how the schematic prediction of Figure 37 and its three tractographic segments are corroborated by Braak's corresponding three histopathologically-confimed

time-wise stages A-B-C of cerebral amyloid spread in AD (Figure 38a). As per his formulation [140]:

- Stage-A mainly involves ventral basal region of temporal and frontal lobes;
- Stage-B chiefly ventral two-thirds of frontal, occipital and parietal (association) regions;
- Stage-C involves remaining regions, primary sensory and motor region in cerebral vertex.

One notes that the Braak stages A-B-C well concurs with tractographic segments1-2-3. Figure 38b shows the corresponding nerve fasciculus obtained by DTI-tracking. Indeed, Segment-1 tracts include the thalamus, and this thalamic involvement in the incipient AD process is corroborated by thalamic morphometry measurements [145]. Furthermore, the circumcerebral aspect of tractographic pathway is also closely substantiated by the circumcerebral Papez circuit-based formulation of AD pathogenesis, supported by electrophysiological and PET-imaging findings [146]. To recollect, the Papez circuit is the C-shaped affective/emotive/memory pathway, traversing entorhinal cortex-prefrontal region-cingulum, and thalamus. Of especial note, is that the dysfunction of dorsal pathway (Segment-3) is corroborated by fMRI and molecular imaging in AD/MCI showing hypoactivation of cingulate region [147, 148]. Indeed, the segments 1-3 correlate respectively with the functional nodes of default-mode network (frontal/parietal/cingulate hubs), and one knows that these hubs become impaired in AD [149].

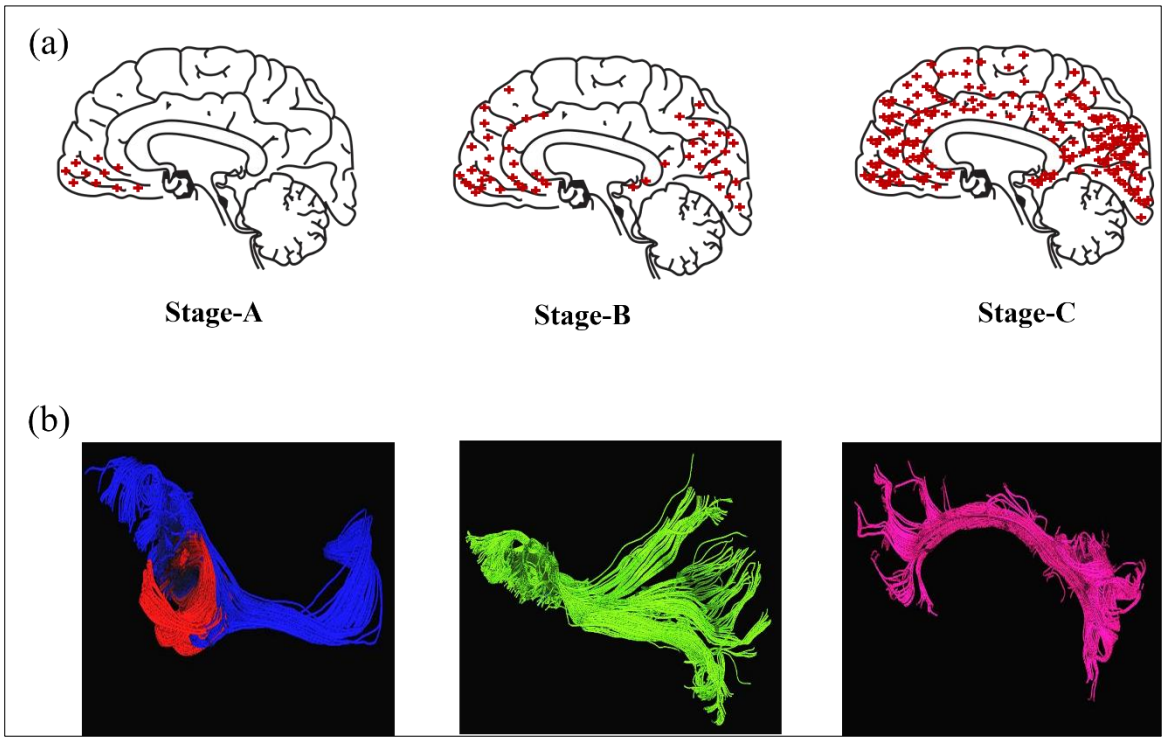

***Figure 38**: (a) Amyloid distribution stages as Alzheimer's disease progresses over time, as observed by microscopic histopathological examination of amyloid plaques denoted by red markings. Braak Stage- A begins with initial amyloid deposits in the isocortex, as the basal zones in frontal and temporal regions. Stage-B shows amyloid gradual spread into ventral two-thirds portion of the frontal, occipital and parietal regions, including the isocortical association areas, except the superior cerebral portion as the sensory and motor regions in the dorsal vertex. Stage-C is late-stage situation where amyloid spreads throughout the cerebral isocotex, including primary sensory and motor region in the cerebral dorsal vertex. (b): The corresponding nerve fasciculus that may act as scaffolds for the amyloid migration, the fasciculus being demarcated by DTI tracking.*

7.3.4 Diffusivity parameters alteration in Alzheimer's Disease

We identified the fibre alteration in the aforementioned tractographic segments 1-3 under AD. We estimated the tract diffusivities (axial/radial/mean-diffusivities) in AD vis-a-vis control subjects (Tables S1-S3). For this comparison, we used diffusion-MRI scans of ten subjects (age-matched/sex-matched five healthy and five AD subjects) from AD Neuroimaging system. We also performed effect-size assessment and power analysis of tract parameters of these subjects and found that the required sample size is four, hence our five subjects of each group would be sufficient for statistical analysis (Figure S2). Indeed,

all the AD vis-à-vis control differences were highly significant (p≈0.005) with large effect-sizes, as shown below.

Using DTI analysis, we found that the tract systems of Segments 1-3 show considerable neural damage in AD with respect to controls. *Segment-1:* Uncinate and orbitofrontal tracts were impaired in AD with significantly higher diffusivity parameters (axial/radial/mean-diffusivities) ($p<0.004$, Figure 39), thus indicating fibre damage and axonal transport impairment. Our observation is correlated by histopathological studies showing that Wallerian-type neuronal degeneration occurs in AD [150]. Nevertheless, the anatomical region of segment-1 improved significantly by metformin treatment in AD ($p=0.044$) [68].

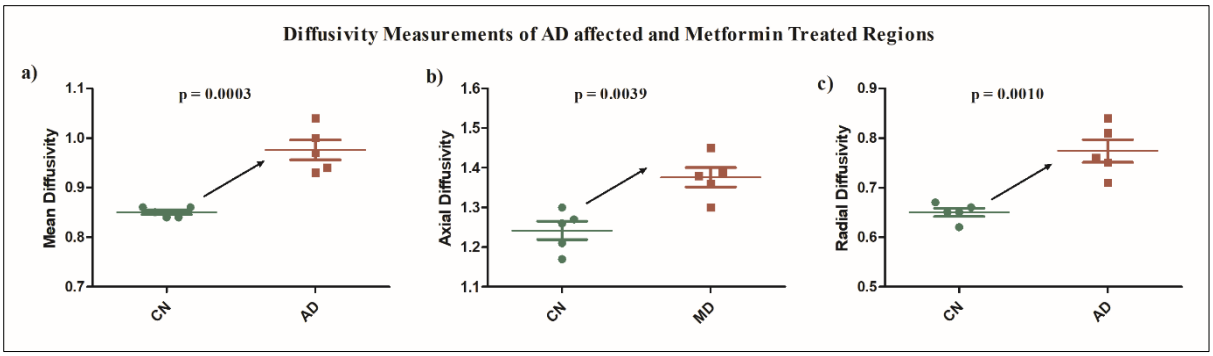

Figure 39: *Neural tract impairment in AD patients at Segment-1 (orbitofrontal and uncinate region): Increase of diffusivity indices in AD subjects over controls: (a) Mean Diffusivity, (b) Axial Diffusivity, and (c) Radial Diffusivity. The p-value is highly significant and there is large effect size.*

Segment-2: Likewise, in AD patients we observed increased diffusivity-based neural tract impairment in the parietal and inferior frontal regions ($p<0.005$; Figure 40). To underscore, the functioning of these regions is enhanced in AD subjects under cilastozol ($p=0.005$) [68].

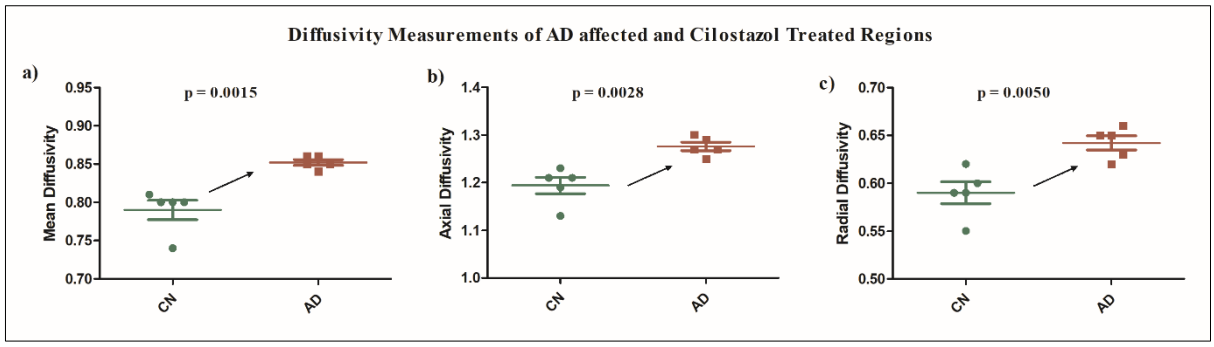

Figure 40: *AD patients show dysfunctionality of fibre tracts at Segment-2 (parietal and inferior frontal regions). There is rise of diffusivity indices in AD subjects over controls: (a) Mean Diffusivity, (b) Axial Diffusivity, and (c) Radial Diffusivity. There is high significance in p-value, with the effect size being large.*

Segment-3: Similarly, we found that fibre dysfunctionality is revealed by higher diffusivities in the posterior cingulate and parietal association regions ($p<0.005$, Figure 41). Moreover, the functionality of these regions improved by rifampicin in AD subjects ($p=0.009$) [65].

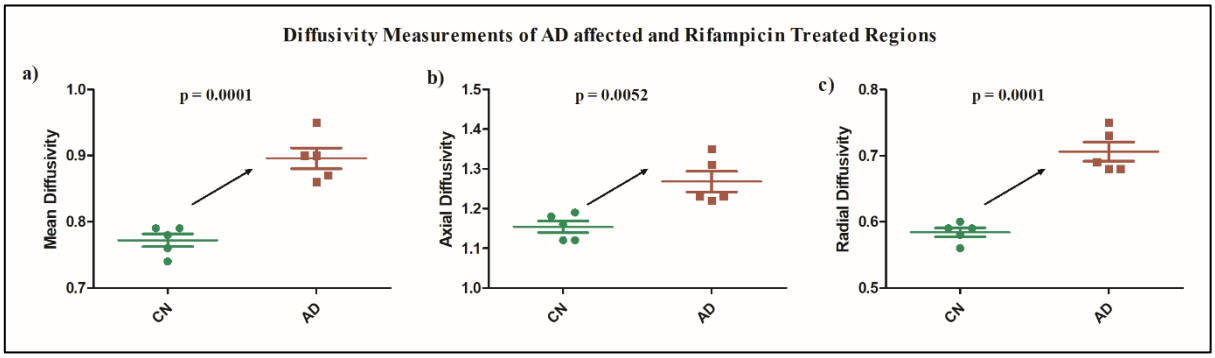

Figure 41: *Dysfunctionality of Neural tract in AD patients at Segment-3 (cingulate and parietal association region): The panels show that diffusivity indices accentuate in AD subjects over controls: (a) Mean Diffusivity, (b) Axial Diffusivity, and (c) Radial Diffusivity. The rise is of high statistical significance ($p\leq0.005$). It may be remarked that the p-value is highly significant, together with large effect size.*

7.3.5 Gene Expression Analysis

We analysed the target genes of the three drugs. We have earlier found that these drugs hepatically excrete amyloid by activating the respective genes- Metformin: ABCB11; Cilostazol: ABCA1/SCD; Rifampicin: MDR1/ABCG2. The expression value of these genes from microarray analysis of autopsy material for normal adults were downloaded from the human brain transcriptome platform of the Allen Brain Atlas (https://human.brain-map.org/). Thereafter, we obtained the required information on the microarray survey, data normalization and platform selection (along with the ontology and nomenclature of neuroanatomical structures of brain) from that atlas platform [Documentation - Allen Human Brain Atlas (brain-map.org)].

We found that these genes are downregulated differentially in separate brain regions. For instance, the gene ABCB11 is downregulated in Segment-1 (and not in segments-2,3). To recall, ABCB11 is metformin's target gene whose expression enables hepatic amyloid-clearance from blood-to-bile via hepatocytes. In AD, this gene may be downregulated and hence metformin may enable upregulation. Further, it is this same gene ABCB11 which is downregulated only in segment-1, the cerebral region which is impaired in AD but can be activated by metformin. Paraphrasing, ABCB11 gene expresses in both liver and cerebral segment-1, and is dysfunctional in AD, and remediation can occur by metformin. Indeed, functioning of the same gene in different tissues may occur by alternative splicing process. To exemplify, the classical fibronectin-FN1 gene can also express in hepatocytes and neurons using differential splicing [150].

We now considered genes ABCA1-SCD (cilostazol). Analysing Allen Brain-Atlas/Human, we found that these genes are downregulated in segment-2 (and not in segments-1,3), where segment-2 is cerebral region activated by cilostazol. Similarly, we

found that genes MDR1-ABCG2 (rifampicin) are downregulated only in segment-3, the region activated by rifampicin. Table 8 summarizes these findings.

7.3.6 Identification of expression of the genes

We see the close correspondence between (i) our systems biology predicted anatomical location of the genes in the circumcerebral region [Segment 1, 2 and 3, vis-à-vis (ii) the microarray based experimental location of the genes. We have considered only the named neuroanatomical structures specified in the circumcerebral region. Hence, we discounted expression of the genes in other brain structures which are outside the circumcerebral region, i.e. we omit the structures as mesencephalon, pons/cerebellum, choroid plexus, habenula (epithalamus), myelencephalon, etc. Likewise, we considered hippocampus proper, i.e. cornu ammonis, and discounted peri-hippocampal structures in the Formatio hippocampi. It is known that such perihippocampal areas are perirhinal cortex, gyrus dentatus and retrohippocampal areas [151]. In Figure S3, the first structure that we identified from the circumcerebral region is the frontal lobe (orbital gyrus, OrG, underlined in Figure S3). This area is located in segment 1.

Similarly, for gene *ABCA1* (Figure S4), we find, from the atlas, that the maximally downregulated value of this gene in the circumcerebral region occurs in hippocampus proper (cornu ammonis, CA2) (underlined in Figure S4). This area correlates with segment-2. Likewise, regarding gene *MDR1*, we observe from the atlas, that the gene's maximally downregulated value in the circumcerebral region occurs in cerebral vertex, i.e. in patietal lobe, namely at paraterminal gyrus that links to supracallosal gyrus and cingulate gyrus. This area corresponds to segment-3. Our overall findings are synoptically illustrated in Table 9 of the text.

7.3.7 Assessment of expression of the genes:

Our analysis revealed that downregulation in segments 1, 2 and 3 respectively corresponds to one gene (*ABCB11*), two genes (*ABCA1*, *SCD*), and two genes (*MDR1*, *ABCG2*). Regarding segment 2, from the microarray measurements of Allen Atlas, we found that *ABCA1* gene was considerably more downregulated than *SCD*. Similarly, regarding segment-3, we noted that *MDR1* was appreciably more downregulated than *ABCG2*. Thus, for the segments 1,2 and 3, we see that the lead genes downregulated are respectively *ABCB11*, *ABCA1* and *MDR1*. From Allen Atlas, we find that these three genes have substantially increased level of down-regulation which is respectively 64%, 165% and 111%. This is shown in Figure 42 of the text.

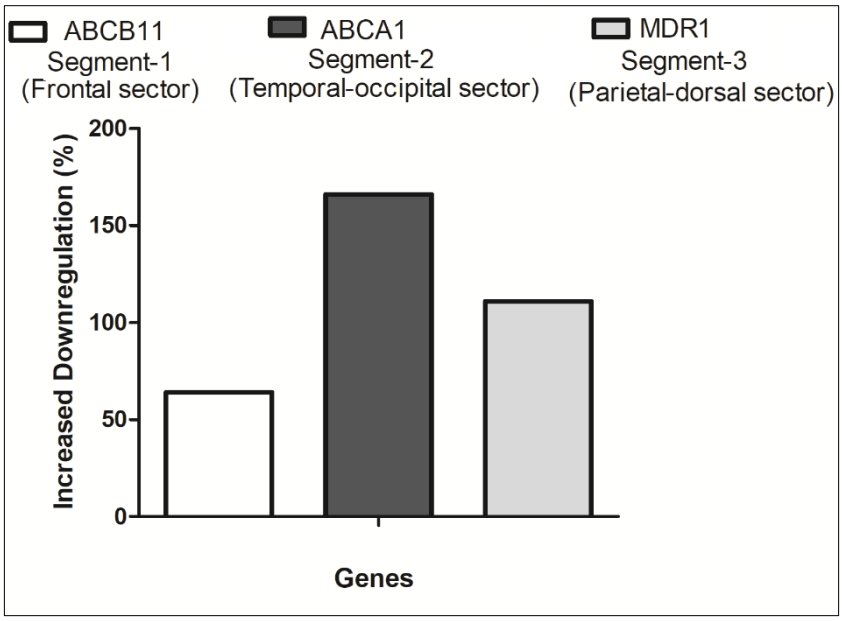

Figure 42: *Intensity of downregulation of the genes ABCB11, ABCA1 and MDR1 respectively in segment 1 (frontal sector), segment 2 (temporal-occipital sector) and segment 3 (parietal-dorsal sector).*

Table 8. Differential gene signatures of the corresponding three neuroanatomical segments that are progressively affected in AD as amyloid spreads in brain (Braak stages A-B-C). Also shown are the respective pharmacological agents and receptors involved in vascular-hepatic elimination of amyloid from those respective segments.

Name of the segment and the hepatomodulatory Drugs	Braak Class	Clinical grading	Name of the tracts	Genes	Brain regions with gene dysregulation
Segment-1: Orbitofrontal cortex-Uncinate fasciculus *Metformin*	Stage A	Prodromal memory dysfunction	Uncinate fasciculus, Anterior thalamic radiation, and Dentetorubot halamic tracts	ABCB11	Frontal lobe
Segment-2: Parietal Lobes-Inferior frontal gyri *Cilostazol*	Stage B	Mild cognitive impairment	Inferior fronto-occipital fasciculus	ABCA1	Temporal lobe (e.g. hippocampus)
				SCD	Temporal lobe (e.g. hippocampus)
Segment-3: Posterior Cingulate Cortex - Parietal Association Cortex *Rifampicin*	Stage C	Alzheimer's Disease	Cingulum fronto-parietal projections, superior longitudinal fasciculus	MDR1	Dorsal vertex region (e.g. cingulate gyrus)
				ABCG2	Dorsal vertex region (e.g. paracentral lobule/ medial sensorimotor area)

7.4 Discussion

In this present study, we aim to clinically validate our previous findings of hepatotropic drugs namely rifampicin, cilostazol and metformin which helps to increase intestinal amyloid-beta excretion and reduce intestinal amyloid-beta reabsorption, by targeting some receptors involved in enterohepatic circulation of amyloid beta. We have showed that our predicted hepatotropic drugs can influence the brain regions impaired in AD. Earlier microscopy based histological research of Braak et al. revealed that limbic, frontal and parietal networks were the preferred circuits affected by amyloid deposition. These networks were also activated by our predicted repurposed drugs in Alzheimer's patients.

Our findings thus imply an innovative pharmaco-anatomical approach to AD management using a neuroanatomical tract-network perspective. Amyloid is majorly cleared by faecal route: brain-amyloid→cerebral blood→liver→bile→faeces, the first and third arrows denoting cellular-efflux interfaces (neurovascular pericytes, and hepatocytes respectively). These various alternative amyloid-efflux pathways and gene-sets are expressed at both interfaces, respectively in the brain and the liver [86], thereby enabling seamless integrated amyloid-excretion route. Different brain regions may involve different signalling pathways which may be enhanced by the corresponding drugs that we have indicated (Figure 43).

It is known that AD has chiefly four different biological sub-types as frontal, temporal, parietal, and diffuse-atrophy types [86]. The first three sub-types thus neuroanatomically relates to neuroanatomical segments-1,2,3 respectively. Hence, our analysis implies that these three types may be respectively suitable for metformin, cilasatozol and rifampicin. However, the diffuse-atrophy type is generalized anatomically across the cerebrum and so may be feasible for all the three drugs combined synergistically

(Table 9). Thus, we observe a novel potential of hepatomodulative amyloid-excreting drugs towards neuroanatomically-based personalized therapeutic approach to AD, adapted according to the individual biological subtypes of AD that the patient posseses.

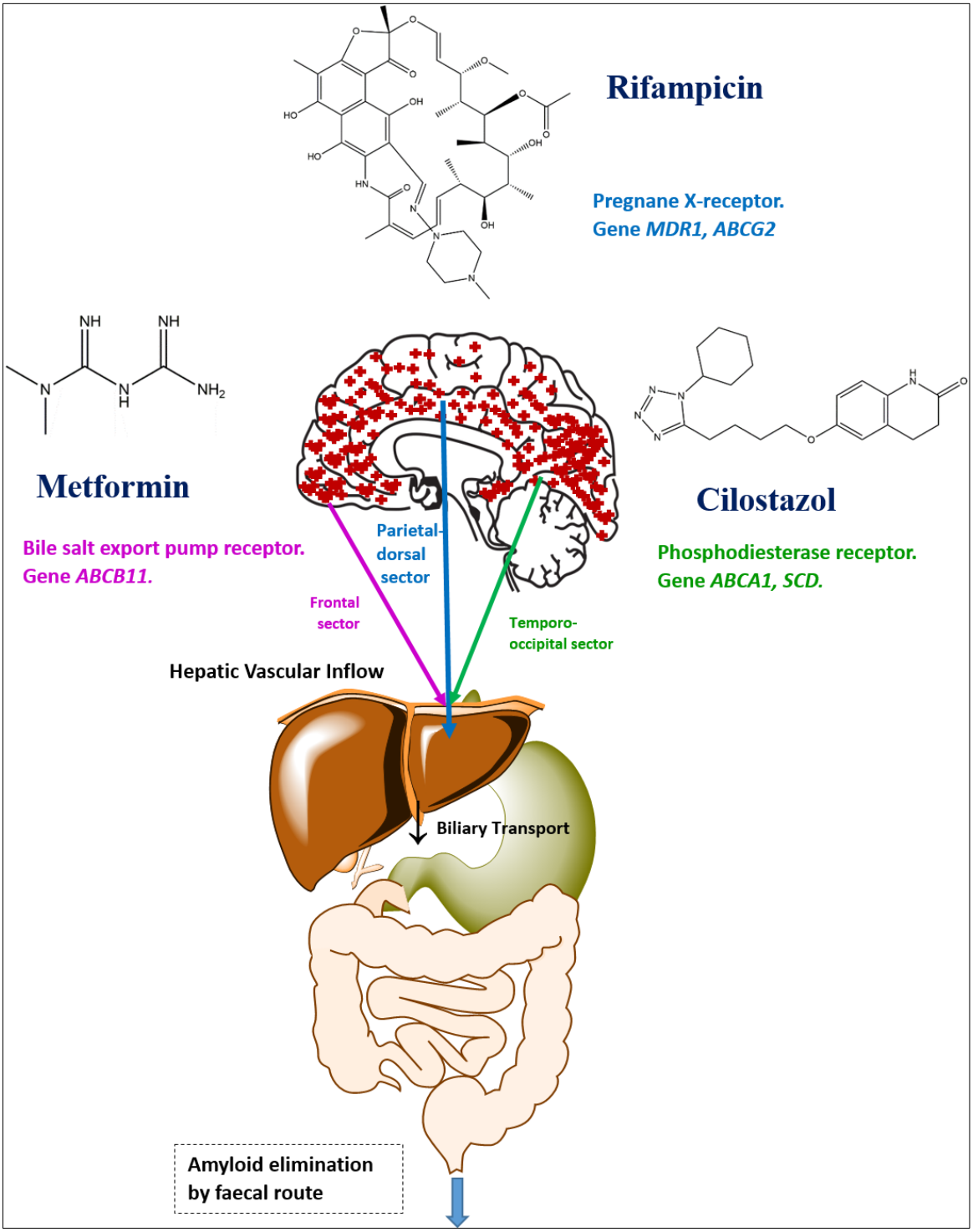

***Figure 43**: Physiological routes, receptors and pharmacomodulation of hepatic clearance of amyloid from different brain regions.*

Previous research has identified the posterior cingulate cortex network as the most vulnerable epicentre for AD and also responsible for its progression [152]. The other vulnerable regions are parietal and frontal lobes. Hoesen et al., reported that the orbitofrontal cortex exhibits a significant amount of neurofibrillary tangle in AD [153]. Several studies also reported diffusion abnormalities of the uncinate fasciculus in AD [154]. In this present study we aim to identify the tracts between the brain regions which are affected in AD and treatment with the proposed hepatomodulative drugs improve the glucose metabolism of these regions. This reduction in cerebral glucose metabolism occurs prior to pathology and symptom manifestation, persists as symptoms progress, and is more severe than normal ageing [155]. Therefore, evaluating the white matter integrity in these areas may help in the early screening of AD.

To sum up, we may highlight that our analysis indicates a novel potential of hepatomodulative amyloid-excreting drugs towards a neuroanatomically-based therapeutic approach to AD depending on the biological variant or subtype of AD. It is well known that AD is actually a multi-phenotype based gamut of biological neurodegenerative behaviour, constituting the Alzheimer's Syndrome spectrum, and the therapeutic response critically depends of the phenotypic subtype of AD [156]. Since conventional therapies aimed at cerebral amyloid formation do not always have the desired effect in AD, it may be imperative to probe collateral avenues. The recent multisystemic perspective of dementia delineates that AD is a hepatic metabolic encephalopathy [157], and this can furnish a unique prospect of intervening in AD from an metabolic angle.

Table 9. Biological subtypes of AD and corresponding possible anatomically-based personalized pharmacological enhancement of amyloid elimination for the subtypes.

Alzheimer's Disease Biological Subtype	Brain regions involved	Anatomical segments associated	Feasibility of hepatomodulative drug
Frontal subtype	Lateral frontal region	Segment-1	Metformin
Temporal subtype	Middle and inferior temporal region	Segment-2	Cilostazol
Parietal subtype	Lateral parietal, precuneus and cingulate region	Segment-3	Rifampicin
Diffuse atrophy subtype	Nearly all regions	All three segments	Combination: Metformin, Cilostazol, Rifampicin

7.5 Conclusion

In conclusion, we have approached a therapeutic perspective to Alzheimer's disease from one of its basic initial pathophysiological processes, namely as hepatic metabolic dysfunction affecting the brain, reminiscent of the generalized systems approach of metabolic encepahalopathies. Our neuroanatomical tractographic analysis, as far as we know, is the first pilot study in this direction. We thus observe the possibility of amyloid-clearing hepatomodulative drugs as a novel substantive therapeutic approach to Alzheimer's disease, and the potentiality of these drugs targeting the corresponding different affected tract networks. Furthermore, multidrug combination therapy may target all three different brain networks (fronto-parietal, occipito-cingular and limbic) at the same time and could be an effective synergistic approach for Alzheimer's therapy.